



A neutron diffraction and NMR study of ferroelectric and antiferroelectric ordering in  $\text{CsH}_2\text{PO}_4$  at high pressure  
by Paul John Schuele

A thesis submitted in partial fulfillment of the requirements for the degree of Doctor of Philosophy in Physics  
Montana State University  
© Copyright by Paul John Schuele (1988)

Abstract:

A fully three dimensional neutron diffraction study has been carried out on  $\text{CSH}_2\text{PO}_4$  in the pressure induced antiferroelectric phase. At 100.0 K and a hydrostatic pressure of 3.6 kbar the structural parameters are  $a = 15.625(9)$ ,  $b = 6.254(2)$ ,  $c = 4.886(1)$  Å,  $\gamma' = 108.08(3)^\circ$  and  $Z = 4$ . Atomic positions and thermal parameters were determined using full-matrix least-squares methods which yield final agreements of  $R_w(F^2) = 0.0793$  for space group  $P2_1$  and  $R_w(F_z) = 0.0829$  in space group  $P2_1/a$ . Hydrogens bonding in b-chains, which are disordered in the paraelectric phase, show antiferroelectric ordering such that ferroelectrically ordered b-axis chains are arranged in ferroelectric b-c planes with neighboring planes in the a direction ordered in the opposite sense. This ordering leads to a doubling of the structure along the a axis.

A high-pressure low-temperature nuclear magnetic resonance apparatus was constructed to investigate the dynamics of the phase transitions in  $\text{CSH}_2\text{PO}_4$ . This apparatus was used to measure the  $^{133}\text{Cs}$  spin-lattice relaxation time in the paraelectric phase at pressures of 0.001, 1.5, 3.0, 3.3 and 3.6 kbar. Relaxation data were interpreted in terms of a pseudo-Ising model yielding a correlation time for cesium motions of  $1.0 \times 10^{-12}$  seconds. Interaction strengths and pressure dependences along each principal axis were found to be  $J_b/k = 266.0 \text{ K} - 12.0 \text{ K/kbar} * P$ ,  $J_c/k = 2.1 \text{ K} - 0.13 \text{ K/kbar} * P$  and  $J_a/k = 0.3 \text{ K} - 0.09 \text{ K/kbar} * P$ .

Based on the resonance results a second antiferroelectric phase is predicted at pressures above 16.2 kbar and temperatures below 38 K. For this phase each ordered b-axis H-bond chain would have four nearest neighbor chains ordered in the opposite sense.

A NEUTRON DIFFRACTION AND NMR STUDY OF FERROELECTRIC AND  
ANTIFERROELECTRIC ORDERING IN  $\text{CsH}_2\text{PO}_4$  AT HIGH PRESSURE

by

Paul John Schuele

A thesis submitted in partial fulfillment  
of the requirements for the degree

of

Doctor of Philosophy

in

Physics

MONTANA STATE UNIVERSITY  
Bozeman, Montana

March 1988

78  
4792

APPROVAL

of a thesis submitted by

Paul John Schuele

This thesis has been read by each member of the thesis committee and has been found to be satisfactory regarding content, English usage, format, citations, bibliographic style, and consistency, and is ready for submission to the College of Graduate Studies.

March 2, 1988  
Date

V. Hugo Schmidt  
Chairperson,  
Graduate Committee

Approved for the Major Department

March 2, 1988  
Date

W. H. Jensen  
Head, Major Department

Approved for the College of Graduate Studies

3-11-88  
Date

W. B. Malone  
Graduate Dean

## STATEMENT OF PERMISSION TO USE

In presenting this thesis in partial fulfillment of the requirements for a doctoral degree at Montana State University, I agree that the Library shall make it available to borrowers under rules of the Library. I further agree that copying of this thesis is allowable only for scholarly purposes, consistent with "fair use" as prescribed in the U.S. Copyright Law. Requests for extensive copying or reproduction of this thesis should be referred to University Microfilms International, 300 North Zeeb Road, Ann Arbor, Michigan 48106, to whom I have granted "the exclusive right to reproduce and distribute copies of the dissertation in and from microfilm and the right to reproduce and distribute by abstract in any format."

Signature Paul John Schulte

Date March 2, 1988

## ACKNOWLEDGMENT

I would like to thank my parents and family for their unflinching support during the course of this work. I am grateful for the technical guidance of Dr. V. Hugo Schmidt and Dr. Robert Thomas. Several expert technicians including A. Beldring, T. Jungst and T. Knick at Montana State University and J. Henriques at Brookhaven National Laboratory contributed to the construction and repair of experimental apparatus. I would also like to thank the faculty and graduate students of the Physics Department for their freely given support. In particular Paul Schnackenberg, Dr. John Drumheller and Dr. George Tuthill assisted with technical and personal aspects of this work.

The neutron diffraction experiment was performed at Brookhaven National Laboratory under U. S. Department of Energy contract DE-AC02-76CH00016. I gratefully acknowledge financial support from a Walter C. Hamilton Fellowship at Brookhaven National Laboratory and National Science Foundation grants at Montana State University.

Finally I would like to express my deep gratitude to Jeannette Fiore for her love and understanding. A solid emotional anchor has been the most important thing of all.

## TABLE OF CONTENTS

	Page
LIST OF TABLES.....	vii
LIST OF FIGURES.....	viii
ABSTRACT.....	x
1. INTRODUCTION TO THE PHASE TRANSITIONS IN $\text{CsH}_2\text{PO}_4$ ..	1
Introduction.....	1
Previous Experimental Results for CDP.....	6
Theory of the Phase Transitions in CDP.....	21
The Present Investigation.....	29
2. NEUTRON DIFFRACTION DETERMINATION OF THE ANTIFERROELECTRIC PHASE STRUCTURE.....	31
Introduction.....	31
Experimental.....	33
Data Reduction.....	41
Structure Refinement.....	44
Discussion.....	52
3. HIGH PRESSURE LOW TEMPERATURE NMR APPARATUS.....	62
Introduction.....	62
Apparatus Description.....	67
High Pressure Electrical Feedthroughs.....	73
High Pressure Generation System.....	75
Design and Construction of NMR Sample Coils.....	78
Technique for Concurrent Dielectric Measurements.....	83
4. NMR MEASUREMENT OF THE $^{133}\text{Cs}$ SPIN-LATTICE RELAXATION TIME AS A FUNCTION OF TEMPERATURE AND PRESSURE.....	84
Introduction.....	84
Experimental.....	84
Measurement Technique.....	88
Experimental Results.....	93

TABLE OF CONTENTS--Continued

	Page
5. THEORETICAL ANALYSIS OF $^{133}\text{Cs}$ SPIN-LATTICE RELAXATION TIME DATA.....	102
Introduction.....	102
Relaxation Theory for the Case of CDP.....	103
Data Analysis.....	113
Discussion.....	115
6. CONCLUSION.....	122
LITERATURE CITED.....	125
APPENDIX--SPIN-LATTICE RELAXATION DATA FOR CDP.....	131

## LIST OF TABLES

Table	Page
1. Atomic Displacements in CDP Due to the Ferroelectric Mode From Neutron Scattering.....	13
2. Interaction Strengths in CDP and DCDP from Published Literature.....	17
3. Crystal Data for CDP from Neutron Diffraction.....	38
4. Details of Neutron Diffraction Experiment.....	40
5. Results of Alternate Structural Models for the Antiferroelectric Phase of CDP.....	51
6. Positional Parameters for Space Group $P2_1$ .....	53
7. Thermal Parameters for Space Group $P2_1$ .....	54
8. Positional Parameters for Space Group $P2_1/a$ .....	55
9. Thermal Parameters for Space Group $P2_1/a$ .....	56
10. Distance and Angles for Hydrogen Bonds In Paraelectric, Ferroelectric and Antiferroelectric phases.....	59
11. Distance and Angles for $PO_4$ Groups In Paraelectric, Ferroelectric and Antiferroelectric phases.....	60
12. Spin-Lattice-Relaxation Data for $^{133}Cs$ at 1 bar Pressure.....	132
13. Spin-Lattice-Relaxation Data for $^{133}Cs$ at 1.5 kbar Pressure.....	133
14. Spin-Lattice-Relaxation Data for $^{133}Cs$ at 3.0 kbar Pressure.....	134
15. Spin-Lattice-Relaxation Data for $^{133}Cs$ at 3.3 kbar Pressure.....	135
16. Spin-Lattice-Relaxation Data for $^{133}Cs$ at 3.6 kbar Pressure.....	136



## LIST OF FIGURES

Figure	Page
1. Schematic Representation of Ordering Due to Phase Transitions.....	5
2. Phase Diagram for $\text{CsH}_2\text{PO}_4$ .....	7
3. Crystal Structure of $\text{CsH}_2\text{PO}_4$ .....	10
4. Pressure Vessel for Neutron Diffraction.....	35
5. Schematic of a Four-circle Diffractometer.....	36
6. Block Diagram of the Basic NMR Experiment.....	65
7. High Pressure Vessel and Cryostat.....	68
8. Pressure Vessel Seal and Electrical Feedthrough...	72
9. High Pressure Generation Apparatus.....	76
10. NMR Pulse Sequence and Typical Free Induction Decay Signal.....	89
11. A Typical Plot of FID Amplitude Versus Recovery Time.....	91
12. Spin Lattice Relaxation Rate for CDP at 1 bar Pressure.....	94
13. Spin Lattice Relaxation Rate for CDP at 1.5 kbar Pressure.....	96
14. Spin Lattice Relaxation Rate for CDP at 3.0 kbar Pressure.....	98
15. Spin Lattice Relaxation Rate for CDP at 3.3 kbar Pressure.....	99
16. Spin Lattice Relaxation Rate for CDP at 3.6 kbar Pressure.....	100

LIST OF FIGURES--Continued

Figure	Page
17. Critical Spin Lattice Relaxation Rate for CDP at 1 bar Pressure with Theoretical Fit.....	116
18. Critical Spin Lattice Relaxation Rate for CDP at 1.5 kbar Pressure with Theoretical Fit.....	117
19. Critical Spin Lattice Relaxation Rate for CDP at 3.0 kbar Pressure with Theoretical Fit.....	118
20. Critical Spin Lattice Relaxation Rate for CDP at 3.3 kbar Pressure with Theoretical Fit.....	119
21. Critical Spin Lattice Relaxation Rate for CDP at 3.6 kbar Pressure with Theoretical Fit.....	120

## ABSTRACT

A fully three dimensional neutron diffraction study has been carried out on  $\text{CsH}_2\text{PO}_4$  in the pressure induced antiferroelectric phase. At 100.0 K and a hydrostatic pressure of 3.6 kbar the structural parameters are  $a = 15.625(9)$ ,  $b = 6.254(2)$ ,  $c = 4.886(1)$  Å,  $\gamma = 108.08(3)^\circ$  and  $Z = 4$ . Atomic positions and thermal parameters were determined using full-matrix least-squares methods which yield final agreements of  $R_w(F^2) = 0.0793$  for space group  $P2_1$  and  $R_w(F^2) = 0.0829$  in space group  $P2_1/a$ . Hydrogens bonding in b-chains, which are disordered in the paraelectric phase, show antiferroelectric ordering such that ferroelectrically ordered b-axis chains are arranged in ferroelectric b-c planes with neighboring planes in the a direction ordered in the opposite sense. This ordering leads to a doubling of the structure along the a axis.

A high-pressure low-temperature nuclear magnetic resonance apparatus was constructed to investigate the dynamics of the phase transitions in  $\text{CsH}_2\text{PO}_4$ . This apparatus was used to measure the  $^{133}\text{Cs}$  spin-lattice relaxation time in the paraelectric phase at pressures of 0.001, 1.5, 3.0, 3.3 and 3.6 kbar. Relaxation data were interpreted in terms of a pseudo-Ising model yielding a correlation time for cesium motions of  $1.0 \times 10^{-12}$  seconds. Interaction strengths and pressure dependences along each principal axis were found to be  $J_b/k = 266.0 \text{ K} - 12.0 \text{ K/kbar} * P$ ,  $J_c/k = 2.1 \text{ K} - 0.13 \text{ K/kbar} * P$  and  $J_a/k = 0.3 \text{ K} - 0.09 \text{ K/kbar} * P$ .

Based on the resonance results a second antiferroelectric phase is predicted at pressures above 16.2 kbar and temperatures below 38 K. For this phase each ordered b-axis H-bond chain would have four nearest neighbor chains ordered in the opposite sense.

## CHAPTER 1

INTRODUCTION TO THE PHASE TRANSITIONS IN  $\text{CsH}_2\text{PO}_4$ Introduction

For many years the study of structural phase transitions has made up a considerable portion of the work done in solid state physics. This interest is quite natural in light of the profound changes in the physical properties of a material which can be induced by small changes in extensive variables such as temperature, pressure or externally applied fields. Of the very large number of solids which undergo structural phase transitions, one important subset is the group of materials with ferroelectric (FE) or antiferroelectric (AFE) transitions.

From a crystallographic perspective all single crystalline solids can be assigned to one of 32 crystal classes, eleven of which are centrosymmetric and thus nonpolar. Of the remaining 21 noncentrosymmetric crystal classes 20 are piezoelectric. A piezoelectric crystal gains an electrical polarization when a mechanical stress is applied and is subject to mechanical strain when an external electric field is applied. Ten of the

piezoelectric crystal classes also possess a spontaneous polarization which can be expressed as an electric dipole moment per unit volume. The spontaneous polarization of polar systems is a function of temperature so a current can be generated by these materials as temperature is varied. Thus these crystals are also referred to as pyroelectric.

Some pyroelectric crystals are also ferroelectric. A ferroelectric crystal is one which has two possible electrically polar equilibrium states which can be reversed by an externally applied electric field. These states have the same crystal structure and differ only in the direction of the electric polarization vector. It is almost always the case that a ferroelectric phase occurs as a small structural distortion of a nonferroelectric prototype phase having higher symmetry. If no spontaneous polarization is associated with the transition the low temperature phase is said to be ferrodistoritive.

A ferroelectric system has a spontaneous polarization  $P_s$  which decreases with increasing temperature and disappears at the structural phase transition to the high temperature paraelectric phase. This transition temperature is known as the Curie temperature  $T_c$ . If the spontaneous polarization decreases to zero continuously on approaching  $T_c$  from below the phase transition is

categorized as second order. For a first order transition  $P_s$  goes to zero discontinuously at  $T_c$ . Clearly the spontaneous polarization is the order parameter for the ferroelectric phase. In the paraelectric phase the dielectric permittivity  $\epsilon$  diverges following the Curie-Weiss law

$$\epsilon = \frac{C}{(T - T_0)}$$

on approaching the transition temperature. Here  $T_0$  is the Curie-Weiss temperature which is equal to  $T_c$  for second order transitions and less than  $T_c$  for first order transitions. It can be seen that the static properties of ferroelectric transitions can be investigated by dielectric measurements of Curie-Weiss behavior in the paraelectric phase and measurements of the spontaneous polarization in the ferroelectric phase.

It is also possible for a paraelectric phase to undergo a transition to an antidistortive phase. In this case the prototype phase unit cell doubles at  $T_c$  due to oppositely directed distortions in adjacent unit cells. If the distortion involves displacements of charged groups to produce polarization the resulting phase is antipolar. The antipolar phase unit cell is made up of two prototype phase unit cells with spontaneous polarizations of equal

magnitude in opposite directions. Thus the effect of these sublattice polarizations is to produce a phase having zero net polarization. Antiferroelectric systems make up a subclass of the antipolar phases which can be forced into ferroelectric order by the application of an external electric field larger than the coercive field. Figure 1 shows a schematic view of the distortions associated with each type of phase transition.

The dynamic behavior at paraelectric to ferroelectric and paraelectric to antiferroelectric phase transitions is associated with the condensation of a lattice vibration mode which conforms to the structural distortion of the low temperature phase. The frequency of this soft mode decreases as the transition is approached from above until it freezes in at the transition temperature. For ferroelectric transitions the soft mode condenses at the center of the Brillouin zone. For antiferroelectric transitions which yield a cell doubling the soft mode condensation takes place at the Brillouin zone boundary of the high temperature phase. This characteristic slowing of a phonon mode can be monitored by means of nuclear magnetic resonance and neutron scattering among other techniques.

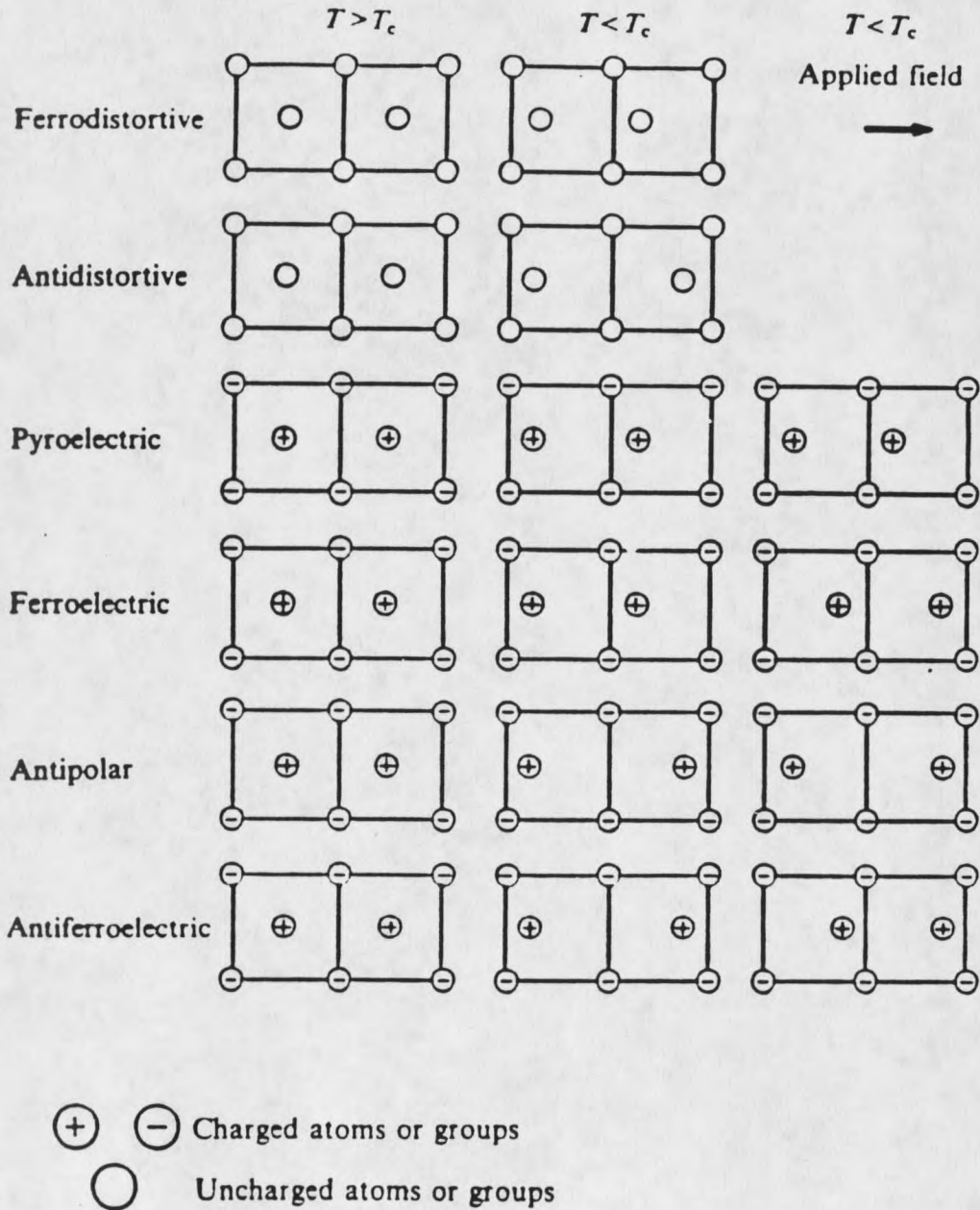


Figure 1. A schematic representation of common phase transition types showing the distortion from the prototype phase.



A comprehensive summary of recent work on ferroelectric and antiferroelectric materials has been presented by Lines and Glass.<sup>1</sup> Older reviews by Jona and Shirane<sup>2</sup> and by Fatuzzo and Merz<sup>3</sup> are also useful. An introduction to phase transitions by Stanley<sup>4</sup> covers the general properties of phase transitions and much of that development can be applied to ferroelectric and antiferroelectric phase transitions.

#### Previous Experimental Results for $\text{CsH}_2\text{PO}_4$

Cesium dihydrogen phosphate,  $\text{CsH}_2\text{PO}_4$  (hereafter referred to as CDP), is a hydrogen bonded system which is paraelectric at room temperature and undergoes a ferroelectric phase transition at 153 K.<sup>5</sup> Unlike  $\text{KH}_2\text{PO}_4$  (KDP) and ferroelectrics isostructural with it, CDP has a third antiferroelectric phase which has been observed by dielectric measurements<sup>6</sup> for temperatures below 124.6(2) K and pressure greater than 3.3(2) kbar. The paraelectric-ferroelectric and paraelectric-antiferroelectric phase boundaries have pressure derivatives of  $dT_c/dP = -8.5$  and  $dT_n/dP = -6.7$  K/kbar respectively. The pressure-temperature phase diagram for CDP, which has been derived from dielectric measurements,<sup>6</sup> is shown in Figure 2.

The phase space of CDP has also been investigated at temperatures from 50 to 450°C and pressures as high as 45

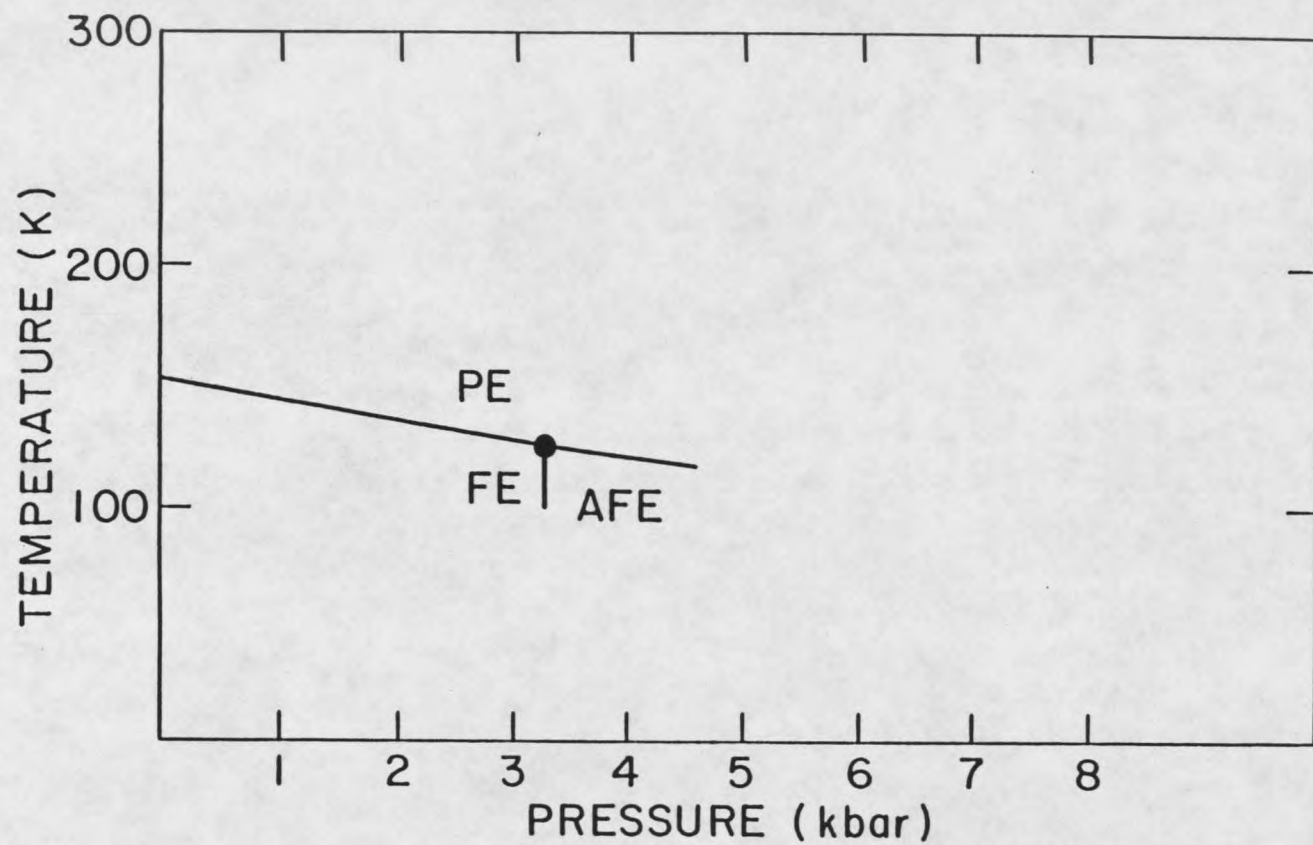


Figure 2. Pressure-temperature phase diagram for  $\text{CsH}_2\text{PO}_4$ . The triple point occurs at  $T = 124.6$  K and  $P = 3.3$  kbar.

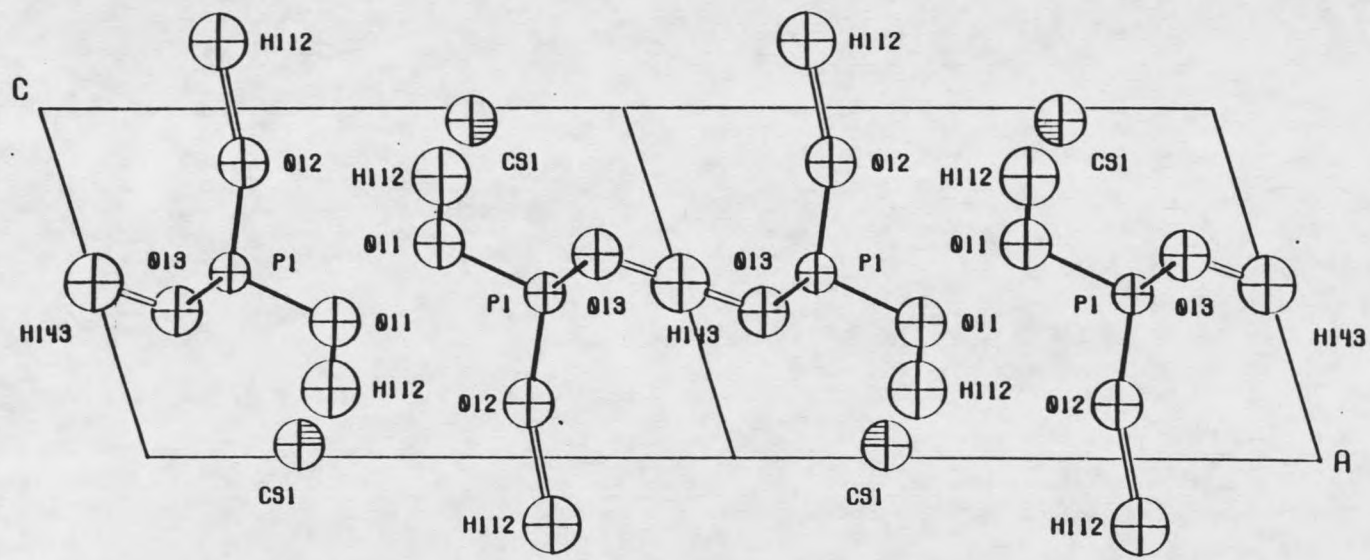
kbar by means of differential scanning calorimetry.<sup>7</sup> These experiments revealed four new phases in addition to the paraelectric phase observed at ambient temperature and pressure. The current work is entirely devoted to the investigation of the three known phases of CDP which occur at or below room temperature.

The deuterated isomorph of CDP,  $\text{CsD}_2\text{PO}_4$  or DCDP, has a similar pressure-temperature phase space but the transitions occur at much higher temperatures. At atmospheric pressure the paraelectric-ferroelectric transition occurs at  $T_c = 267(3)$  K and the pressure derivative of  $T_c$  is  $-8.5(3)$  K/kbar. The triple point between PE, FE and AFE phases is at a temperature of  $218.0(3)$  K and  $P = 5.2(2)$  kbar. Above the triple point the PE-AFE phase boundary has a pressure derivative equal to  $-2.5$  K/kbar. CDP and the deuterated isomorph have the same FE phase structure (space group  $P2_1$ )<sup>8</sup> but the large difference in transition temperatures ( $T_c = 153$  K for CDP and  $T_c = 267$  K for DCDP) indicates that the nature of the hydrogen bonding plays a key role in the phase transition.

At room temperature CDP is monoclinic (space group  $P2_1/m$ ) with two formula units per unit cell.<sup>9</sup> Cesium atoms and  $\text{PO}_4$  groups are centered on mirror planes perpendicular to the b axis at the fractional coordinates  $y = 1/4$  and  $3/4$ . Phosphate groups are linked together by

hydrogen bonds of two inequivalent types; hydrogens in bonds approximately parallel to the c axis are ordered in off center sites in the hydrogen bond, while hydrogens linking phosphate groups in zig-zag chains along the b axis are positionally disordered in double minimum potential wells similar to those found in KDP.<sup>10</sup> The hydrogen bond is usually represented in the literature as  $O-H\cdots O$  and that convention will be followed henceforth. In addition we will use the nomenclature adopted by previous workers which identifies the c-chain hydrogen bond as  $O-H(1)\cdots O$  and the b-chain bond as  $O-H(2)\cdots O$ . The b-chain hydrogen positions were obtained from a refinement of neutron diffraction data with two half occupancy hydrogens placed symmetrically about the center of symmetry at  $(0, 1/2, 1/2)$ . The positions determined were separated by  $0.49 \text{ \AA}$ . A projection of the paraelectric phase structure<sup>9</sup> on the a-c plane is shown in Figure 3.

Upon cooling through the ferroelectric transition the b-chain hydrogens<sup>11</sup> (or deuterons<sup>8</sup>) order in one of the possible off center sites in the  $O-H(2)\cdots O$  bond while the positions of c-chain hydrogens are unaffected. This ordering is accompanied by a relative shift of  $Cs^+$  and  $PO_4^{3-}$  groups along the b axis which produces a spontaneous polarization along the b axis and removes the mirror symmetry plane of the paraelectric phase.



10

Figure 3. The crystal structure of  $\text{CsH}_2\text{PO}_4$  viewed in projection on the a-c plane. Two unit cells along a are shown.

As the transition temperature is approached in the prototype phase, local areas of long range correlation build up which break the symmetry of the high temperature phase and reflect the structure of the ordered phase. In a neutron diffraction experiment these precursor motions cause diffuse distributions of scattered neutrons in addition to the Bragg reflections which are representative of the high temperature phase structure. This diffuse scattering increases in intensity as the sample temperature approaches  $T_c$  and, as correlation lengths increase with decreasing temperature, the scattering distribution becomes more sharply peaked. Thus quasielastic neutron scattering is a powerful method for investigating the dynamics of structural phase transitions which yields the correlation length for ordering as a function of temperature.

The ferroelectric transitions for both CDP<sup>12</sup> and DCDP<sup>12,13,14</sup> have been investigated by means of neutron scattering. For DCDP strong quasielastic scattering was observed in narrow reciprocal space planes perpendicular to the ferroelectric axis which indicates that correlations are strongly one dimensional. Analysis<sup>13</sup> of the data yielded a correlation length of 600 Å along the b axis at  $T_c + 0.3$  K. At that temperature the correlation length along the a and c axes is only about 30 Å. Because

the lattice dimensions differ the correlation extends over about six chains in the *c* direction versus three chains in the *a* direction. Thus interactions within a chain are much stronger than those perpendicular to the chains and the interaction between chains linked by hydrogen bonds along the *c* axis are about twice as strong as those between adjacent chains in the *a* direction. As the temperature is increased correlations along *a* and *c* diminish rapidly while the correlation length along *b* decreases more slowly. At 50 K above  $T_c$  the correlation length along the *b* axis is still about 140 Å.

Calculations based on a simple chain model using the hypothesized ferroelectric mode atomic displacements in Table 1. produced an acceptable fit to neutron scattering data.<sup>12</sup> The largest displacement is of the deuteron in the O(3)-D(1)···O(4) bond from a central position to one close to O(4). In addition it can be seen that cesium atoms and PO<sub>4</sub> groups move toward each other in the *y* direction breaking the mirror plane symmetry of the paraelectric phase and creating a polarization along the *b* axis. There is also a significant deformation of the PO<sub>4</sub> tetrahedron due to the ordering of *b*-chain deuterons which is analogous to that seen in the case of KDP.<sup>15</sup> For DCDF P-O(1) and P-O(2) distances (1.57 Å and 1.49 Å respectively) are essentially unchanged because the

ordering of D(2) atoms is unaffected by the transition. The P-O(3) and P-O(4) bonds are crystallographically equivalent in the paraelectric phase with a length of 1.53 Å. The displacements of Table 1 produce bond lengths of  $d_{P-O(3)} = 1.61 \text{ Å}$  and  $d_{P-O(4)} = 1.47 \text{ Å}$ . For both kinds of O-D...O bonds the long P-O distance is associated with the oxygen which is closest to the deuteron.

Table 1. Atomic displacements in Angstroms from the paraelectric phase structure due to the ferroelectric mode of  $\text{CsD}_2\text{PO}_4$  near  $T_C$ . These results were determined by fitting neutron scattering data.<sup>12</sup>

Atom	x	y	z
D(1)	0.198	0.131	-0.001
D(2)	0	0.048	0
Cs	0	-0.038	0
P	0	0.105	0
O(1)	0	0.048	0
O(2)	0	0.048	0
O(3)	0.040	-0.003	-0.0005
O(4)	-0.040	0.003	0.0005



Neutron scattering experiments using  $\text{CsH}_2\text{PO}_4$  are hindered by the very high incoherent background scattering from hydrogen atoms. However, the reported results<sup>12</sup> are qualitatively similar to those summarized above for the deuterated crystal. Once again the correlations associated with the ferroelectric transition are strongly one-dimensional along the b axis. The displacements of Table 1. in a chain model calculation yield theoretical neutron scattering distributions similar to those observed.

Neutron scattering experiments have been carried out as a function of temperature and pressure for DCDP to investigate both ferroelectric and antiferroelectric ordering.<sup>14</sup> For pressures greater than 5.2 kbar, in the paraelectric phase, a diffuse scattering peak is observed for Miller indices  $h = 2n + 1$ . This indicates precursor antiferroelectric ordering which leads to a doubling of the unit cell along the a axis below  $T_n$ . The presence of scattering at half integer reciprocal lattice points is observed at pressures as low as 3.0 kbar for temperatures within a few degrees of  $T_c$ . With increasing pressure the intensity of antiferroelectric mode scattering increases smoothly becoming dominant at the critical pressure  $P_c$ . Thus both ferroelectric and antiferroelectric fluctuations are present near the triple point. At all pressures the

interaction along  $a$  is very weak amounting to a correlation length of only a few lattice constants even very near the critical temperature. Although scattering experiments have not been carried out on CDP at elevated pressure, it is reasonable to expect the dynamics to be qualitatively similar to those for DCDP.

The general properties observed for the CDP system lead to the hypothesis that the ordering transitions can be parameterized by three interaction strengths. The ferroelectric ordering which takes place along  $b$ -axis hydrogen-bond chains is due to the dominant interaction given by  $J_{||}$ . An interaction along the  $c$  axis, given by  $J_c$ , leads to ordered  $b$ - $c$  planes made up of adjacent ferroelectric  $b$ -axis chains. Finally interactions between neighboring chains in the  $a$  direction are given by  $J_a$ . It is clear that  $J_a$  is positive for pressures below 3.3 kbar because ordering in the  $a$  direction is ferroelectric. If the structure doubles along  $a$  in the antiferroelectric phase it seems reasonable to hypothesize that  $J_a$  has a pressure dependence such that it decreases with increasing pressure, passes through zero at about 3.3 kbar and becomes negative for the antiferroelectric phase.

It is generally agreed that  $J_{||}$  is about 100 to 150 times as strong as  $J_c$  and  $J_c$  is in turn about 10 times as

large as  $J_a$ . Because  $J_c \gg J_a$  the interaction perpendicular to the b axis is often expressed as

$$J_{\perp} = 1/2(J_a + J_c) \approx 1/2 J_c.$$

Thus the intrachain and interchain interactions can also be expressed in terms of  $J_{||}$ ,  $J_{\perp}$  and  $\gamma = J_a/J_c$ . Here  $\gamma$  is a measure of the asymmetry between  $J_a$  and  $J_c$ . Values for these interaction strengths can be determined using a variety of methods including neutron scattering, frequency dependent dielectric measurements and nuclear magnetic resonance. Some values for the interaction strengths as determined by various methods have been compiled by Imai<sup>16</sup> and are reproduced here as Table 2.

Several NMR experiments have been carried out on CDP and DCDP at ambient pressure. The quadrupolar splitting of  $^{133}\text{Cs}$  has been measured as a function of temperature for both the ferroelectric and paraelectric phases.<sup>22</sup> In the paraelectric phase the quadrupolar splitting is zero when the crystal a and c axes are perpendicular to the applied static field. For this crystal orientation the  $^{133}\text{Cs}$  NMR response consists of a single Zeeman line which has a well defined spin lattice relaxation time  $T_1$ . This condition was exploited by Blinc et al.<sup>23</sup> to determine the

Table 2. Interaction strengths for the pseudo-1D Ising model from Reference 16. The primary reference is cited in line one. Experimental methods are indicated by the following letter codes: dielectric (D), neutron scattering (N) and calorimetric (C).

Reference	17	18	19	20	21	16
Method	D	N	D	C	D	C
$J_{  }/k$ (K)	505	-	234	278	266	287
CDP $J_{\perp}/k$ (K)	1.8	-	3.4	2.1	3.0	1.9
$J_{\perp}/J_{  }$ ( $\times 10^3$ )	4	-	14.5	7.6	11	6.6
$J_{  }/k$ (K)	683	650	-	535	611	467
DCDP $J_{\perp}/k$ (K)	0.42	1.1	-	2.5	1.1	3.8
$J_{\perp}/J_{  }$ ( $\times 10^3$ )	0.6	1.7	-	4.7	1.8	8.1

correlation time ( $\tau_0$ ) for polarization fluctuations above  $T_c$ . By assuming that  $J_{||}/J_{\perp} = 170$  and  $\gamma = J_c/J_a = 10$  then fitting  $T_1$  data to a pseudo-one-dimensional-Ising model a value for  $\tau_0$  of  $1.7 \times 10^{-15}$  seconds was obtained.

A study of the temperature dependence of the nuclear quadrupole resonance (NQR) spectra of natural abundance  $^{17}\text{O}$  in CDP<sup>24</sup> has shown two sets of lines with different behavior at  $T_c$ . One set of lines, which is attributed to oxygens in  $\text{O-H}(2)\cdots\text{O}$  bonds lying in chains along the b axis, is unsplit above  $T_c$  and split below. The value of the NQR frequency above  $T_c$  is equal to the average of the two frequencies of the split lines below  $T_c$ . This demonstrates that protons in b-chain bonds are positionally disordered in structurally equivalent double potential wells in the paraelectric phase. On passing through the ferroelectric phase transition b-chain protons order in one of the two sites of the paraelectric phase. The second set of NQR lines, attributed to oxygens in  $\text{O-H}(1)\cdots\text{O}$  bonds lying along the c axis, is unchanged on passing through the transition temperature. Thus the ordering of protons in c-axis hydrogen-bonds is unaffected.

For the deuterated crystal the deuteron quadrupole splitting and spin lattice relaxation time have been

measured at atmospheric pressure.<sup>25</sup> The quadrupole splitting results show that b-chain deuterons are positionally disordered about the center of symmetry above  $T_c$  and ordered in one of the off center sites in the hydrogen-bond below  $T_c$ . In addition the  $^2\text{H}$  spin lattice relaxation time decreases critically on approaching  $T_c$  and is very short compared to that of the deuteron in  $\text{KD}_2\text{PO}_4$ .<sup>26</sup> The anomalously small value of  $T_1$  is attributed to the quasi-one-dimensional nature of correlations in CDP. The correlation time obtained for the deuteron intrabond jump time was  $\tau_0 = 0.9 \times 10^{-12}$  seconds. This is comparable to the value of  $\tau_0 = 1.2 \times 10^{-12}$  sec. obtained for DKDP.<sup>26</sup> It should be noted that the theoretical results for the pseudo-one-dimensional Ising model presented in the paper cited above contain several important typographical errors and a conceptually similar derivation in Reference 23 is more nearly correct.

By considering the results of the experiments summarized above we can form a composite picture of the behavior of CDP as a function of temperature and pressure. In the paraelectric phase cesium atoms and  $\text{PO}_4$  groups are centered in a mirror plane perpendicular to the unique b axis which implies that the lattice polarization along the b axis is zero. Hydrogens in the b axis H-bonds are positionally disordered between two positions located

symmetrically about the center of symmetry at the midpoint of the O-H(2)···O bond. As the temperature is lowered, for pressures below 3.3 kbar, the motion of protons within the O-H(2)···O bonds, as well as that of the Cs and PO<sub>4</sub> groups perpendicular to the mirror plane, become strongly correlated in the b direction. Within a few degrees of T<sub>C</sub> correlations perpendicular to the b axis grow until at T<sub>C</sub> the crystal is ordered ferroelectrically. The ferroelectric order is indicated by the appearance of a spontaneous polarization along the b axis with Cs<sup>+</sup> and PO<sub>4</sub><sup>3-</sup> ionic groups displaced in opposite directions from the mirror plane of the paraelectric prototype phase. In addition the protons in O-H(2)···O bonds are ordered with one proton near each PO<sub>4</sub> group.

For pressures above 3.3 kbar the low temperature ordered phase is antiferroelectric. Thus the crystal has no spontaneous polarization below the transition temperature (T<sub>n</sub>) but a polarization can be induced by the application of an electric field greater than the coercive field. It has been hypothesized<sup>12</sup> that this phase is caused by a change of sign in the interaction between neighboring b-axis chains in the a direction. The unit cell would double along the a axis and each half of the unit cell would be ordered ferroelectrically with opposite orientations. This structure would produce two equal and

opposite sublattice polarizations and a spontaneous polarization of zero.

All experimental tests show that the interactions which lead to ordering are strongly one-dimensional. The ferroelectric interaction along the b axis is on the order of 100 times larger than the coupling between neighboring chains. In addition the coupling in the c direction is roughly an order of magnitude stronger than that along the a axis.

#### Theory of the Phase Transitions in CDP

Because of the strongly one-dimensional character of the ferroelectric and antiferroelectric transitions in CDP, theoretical treatments have been dominated by various forms of the pseudo-one-dimensional Ising model.<sup>27</sup> Ordering for a given unit cell (or half of the unit cell in the antiferroelectric phase) is represented by the pseudospin variable  $s_{i,j}$  which takes on the values  $\pm 1$  depending on the polarization of the unit made up of a  $\text{Cs}^+$  ion and a  $\text{PO}_4^{3-}$  group. For hydrogen-bonded ferroelectrics it is usually the case that the ionic polarization of the unit cell is accompanied by ordering of protons in one of two off-center positions in the hydrogen-bonds. Thus the ordered position of a proton can also be represented by the pseudo-spin variable. It is often convenient to think of the pseudo-spin variable as a measure of the proton



ordering but it should not be forgotten that the pseudo-spin is a representation of the ferroelectric distortion of the unit cell from the structure of the prototype phase.

If we assume an interaction between nearest neighbor spins in the same chain with a strength given by  $J_{||}$ , and an interaction between spins in adjacent chains described by the constant  $J_{\perp}$ , the Hamiltonian for the system can be written as<sup>28</sup>

$$H = - \sum_{i,j} [J_{||} s_{i+1,j} s_{ij} + \frac{1}{2} \sum_{m,n} J_{\perp mn} s_{ij} s_{i+m,j+n} + \mu s_{ij} H_{ij}].$$

Here an external field given by  $H_{ij}$  acts on a dipole of moment  $\mu$ . The index  $i$  indicates the location of a spin within a given  $b$ -axis chain and  $j$  identifies the chain. Thus the first summation in the above Hamiltonian is over all sites while the second is over all interchain couplings to the pseudo-spin  $s_{i,j}$ . In the following it is assumed that the intrachain interaction  $J_{||}$  is much greater than  $J_{\perp}$ . This Hamiltonian contains no explicit dynamic behavior so it is also necessary to assume that some additional coupling to the lattice causes spins to flip spontaneously.<sup>29</sup>

The dynamic behavior of a system containing  $J$  parallel chains, each of which contains  $I$  spins, is given by the master equations<sup>22</sup>

$$\begin{aligned} \frac{d}{dt} P(s_{11}, \dots, s_{ij}, \dots, s_{IJ}, t) = & \\ - \sum_{i,j} W_{ij}(s_{11}, \dots, s_{ij}, \dots, s_{IJ}) P(s_{11}, \dots, s_{ij}, \dots, s_{IJ}, t) & \\ + \sum_{i,j} W_{ij}(s_{11}, \dots, -s_{ij}, \dots, s_{IJ}) & \\ * P(s_{11}, \dots, -s_{ij}, \dots, s_{IJ}, t). & \end{aligned}$$

The term  $P(s_{11}, \dots, s_{IJ}, t)$  is the probability that a given spin configuration  $\{s_{11}, \dots, s_{IJ}\}$  occurs and  $W_{ij}(s_{11}, \dots, s_{IJ})$  is the conditional probability per unit time that the spin  $s_{ij}$  changes orientation. It has been demonstrated<sup>30</sup> that the transition probabilities are given by

$$W_{ij}(s_{11}, \dots, s_{IJ}) = (2\tau)^{-1} [1 - s_{ij} \tanh(\mu\beta h_{ij})]$$

where  $\beta = 1/kT$  and the local field at the site  $(i,j)$  is given by:

$$\begin{aligned} h_{ij} = (J_{||}/\mu) (s_{i+1,j} + s_{i-1,j}) & \\ + 1/\mu \sum_{n,m} J_{\perp mn} s_{i+m,j+n} + H_{ij}. & \end{aligned}$$

The parameter  $(2\tau)^{-1}$  is just the probability per unit time

that a pseudo-spin will reorient due to interaction with the lattice.

With the above expression for  $W_{ij}$  and the master equations, the time dependent ensemble average of the spin polarization at site  $(i,j)$  obeys the following differential equation:

$$\tau (d/dt)\langle s_{ij} \rangle = - \langle s_{ij} \rangle + \langle \tanh(\mu\beta h_{ij}) \rangle.$$

Here the ensemble average  $\langle s_{ij} \rangle$  is defined as:

$$\langle s_{ij} \rangle = \sum_{\{s\}} s_{ij} P(s_{11}, \dots, s_{ij}, \dots, s_{IJ}, t)$$

where the summation is taken over all possible spin configurations. Now we can separate  $\langle s_{ij} \rangle$  into a static component  $\bar{s}$ , which is the average equilibrium value of  $s_{ij}$ , and a fluctuating component  $\langle \delta s_{ij} \rangle$ . Thus  $\langle s_{ij} \rangle$  is given by:

$$\langle s_{ij} \rangle = \bar{s} + \langle \delta s_{ij} \rangle$$

with

$$\bar{s} = \begin{cases} 0, & T \geq T_c \\ [1 - (z\beta J_{\perp})^{-2} \exp(-4\beta J_{\parallel})]^{1/2}, & T \leq T_c. \end{cases}$$

Here the number of neighboring chains is specified by the parameter  $z$ . Similarly the local field at the site  $(i,j)$

can be divided into static and time dependent components as:

$$H_{ij}^{\text{eff}}(t) = H_{ij} + \delta H_{ij}^{\text{eff}}(t),$$

where the static component is given by

$$H_{ij} = (J_{||}/\mu) (s_{i+1,j} + s_{i-1,j}) + \bar{s}/\mu \sum_{m,n} J_{\perp m,n},$$

and the time varying component by

$$\delta H_{ij}^{\text{eff}}(t) = H_{ij}(t) + \mu^{-1} \sum_{m,n} J_{\perp m,n} \langle \delta s_{i+m,j+n} \rangle.$$

With these definitions the differential equation for the dynamic behavior of  $\langle \delta s_{ij} \rangle$  becomes:

$$\begin{aligned} \tau (d/dt) \langle \delta s_{ij} \rangle = & -[\langle \delta s_{ij} \rangle - \gamma/2(\langle \delta s_{i+1,j} \rangle + \langle \delta s_{i-1,j} \rangle)] \\ & + \beta\mu(1 - \Theta) \delta H_{ij}^{\text{eff}}(t), \end{aligned}$$

with

$$\Theta = \begin{cases} 1 - 2e^{-2\beta J_{||}} & T \geq T_c \\ 1 - 2(z\beta J_{\perp})^{-3} \exp(-8\beta J_{||}) & T \leq T_c \end{cases}$$

and

$$\gamma = \tanh(2\beta J_{||}).$$

This coupled system of equations can be decoupled by introducing the Fourier transforms of the spin variables

and the effective field as follows:

$$\langle \delta s_{\mathbf{q}} \rangle = \sum_{i,j} \exp[i\mathbf{q} \cdot \mathbf{r}_{ij}] \langle \delta s_{ij} \rangle$$

and

$$H_{\mathbf{q}}^{\text{eff}}(t) = N^{-1} \sum_{i,j} \exp[i\mathbf{q} \cdot \mathbf{r}_{ij}] H_{ij}^{\text{eff}}(t).$$

Thus the differential equation for the time behavior of  $\langle \delta s_{ij} \rangle$  becomes

$$\begin{aligned} \tau \left( \frac{d}{dt} \right) \langle \delta s_{\mathbf{q}} \rangle &= - \langle \delta s_{\mathbf{q}} \rangle + \gamma \cos(\mathbf{q}_{||} d_{||}) \langle \delta s_{\mathbf{q}} \rangle \\ &+ N\beta\mu(1 - \Theta) \delta H_{\mathbf{q}}^{\text{eff}}(t). \end{aligned}$$

The quantity  $\mathbf{q}_{||}$  is the component of the wave vector  $\mathbf{q}$  along the chains and  $d_{||}$  is the distance between adjoining spins in a chain. If we assume a sinusoidal perturbation field  $H_{\mathbf{q}}^{\text{eff}}(t)$ , then the response polarization has the same sinusoidal time dependence and is given by

$$P_{\mathbf{q}}(t) = (\mu/V) \langle \delta s_{\mathbf{q}} \rangle_0 e^{i\omega t}.$$

Here  $V$  is the volume of the system and  $\langle \delta s_{\mathbf{q}} \rangle_0$  is the following solution of the differential equation for  $\langle \delta s_{\mathbf{q}} \rangle$ :

$$\langle \delta s_{\mathbf{q}} \rangle_0 = \frac{N\beta\mu(1 - \Theta)}{1 - \gamma \cos(\mathbf{q}_{||} d_{||}) + i\omega\tau} \delta H_{\mathbf{q}}^{\text{eff}}.$$

If we substitute for  $\langle \delta s_q \rangle_0$  it can be seen that the time dependent polarization assumes the following form:

$$P_q(t) = \text{Re}[X(q, \omega) \delta H_q e^{i\omega t}].$$

Thus we can identify the generalized dynamic susceptibility for the 1-D Ising model as:

$$X_{1-D}(q, \omega) = \frac{X_{1-D}(q, 0)}{1 + i\omega\tau_{1-D} q},$$

where

$$X_{1-D}(q, 0) = n \frac{\mu^2}{kT} \frac{1 - \theta}{1 - \gamma \cos(q_{||} d_{||})}$$

and

$$\tau_{1-D} q = \frac{\tau}{1 - \gamma \cos(q_{||} d_{||})}.$$

Here  $n$  is the spin density while  $\gamma$  and  $\theta$  have been defined above.

Now couplings perpendicular to the chains can be explicitly included by adding the interaction  $J_{\perp}$  in the Fourier transform of the effective field as follows:

$$\delta H_q^{\text{eff}}(t) = \delta H_q(t) + \frac{z}{n\mu^2} J_{\perp}(q) P_q(t).$$

Thus an expression for the response polarization of the

three dimensional system is obtained as follows:

$$P_q(t) = \text{Re}[X_{1-D}(q, \omega) * \{\delta H_q e^{i\omega t} + \frac{z}{n\mu^2} J_{\perp}(q) P_q(t)\}]$$

with a dynamic susceptibility given by

$$X(q, \omega) = \frac{X_{1-D}(q, \omega)}{1 - (z/n\mu^2) X_{1-D}(q, \omega) J_{\perp}(q)}$$

This result can also be expressed using the definition of the 1-D dynamic susceptibility as

$$X(q, \omega) = \frac{X(q, 0)}{1 + i\omega\tau_q}$$

with

$$X(q, 0) = \frac{X_{1-D}(q, 0)}{1 - (z/n\mu^2) X_{1-D}(q, 0) J_{\perp}(q)}$$

and

$$\tau_q = \frac{\tau kT}{n\mu^2(1 - \theta)} X(q, 0).$$

We know that the static susceptibility  $X(0,0)$  is singular at the transition temperature so  $T_c$  can be determined from the equation

$$1 - \frac{zJ_{\perp}(0)}{n\mu^2} X_{1-D}(0,0) = 0$$

which has the approximate solution

$$\frac{zJ_{\perp}(0)}{kT_c} = \exp \frac{-2J_{\parallel}}{kT_c} .$$

It can be seen that the small interaction perpendicular to the chains (given by  $J_{\perp}$ ) causes the ordering transition to take place quite far above zero Kelvin which is the result for a system with strictly one dimensional interactions.<sup>31</sup>

#### The Present Investigation

We have seen above that an understanding of the phase transitions in CDP has been built up piece by piece from the results of many complementary experimental techniques. Because the paraelectric-antiferroelectric phase transition appears only at high pressure, relatively few experiments have been carried out to determine its properties. Thus this work was initiated to expand our knowledge of the pressure and temperature dependence of the ordering in CDP.

The experiments described in the remaining chapters of this work were carried out to investigate two aspects of the phase transitions in CDP. First the structure of the pressure induced antiferroelectric phase was determined from a high-pressure low-temperature neutron diffraction experiment. It is clear that any further



investigation of the antiferroelectric phase would be facilitated by knowledge of this structure. Secondly the  $^{133}\text{Cs}$  spin lattice relaxation time was measured as a function of temperature and pressure to investigate the dynamics of the ordering in CDP as the ferroelectric and antiferroelectric phases are approached in the paraelectric phase. This information, in conjunction with a suitable pseudo-one-dimensional Ising model, was used to extend our understanding of the effect of pressure on the interactions which lead to the ordered state.















































































































































































































































